Strong spin-orbit-induced Gilbert damping and *g*-shift in iron-platinum nanoparticles

Jürgen Kötzler, Detlef Görlitz, and Frank Wiekhorst
Institut für Angewandte Physik und Zentrum für Mikrostrukturforschung, Universität Hamburg, Jungiusstrasse 11, D-20355 Hamburg, Germany

(Received 23 June 2007; revised manuscript received 1 August 2007; published 6 September 2007)

The shape of ferromagnetic resonance spectra of highly dispersed, chemically disordered $Fe_{0.2}Pt_{0.8}$ nanospheres is perfectly described by the solution of the Landau-Lifshitz-Gilbert (LLG) equation excluding effects by crystalline anisotropy and superparamagnetic fluctuations. Upon decreasing temperature, the LLG damping $\alpha(T)$ and a negative g-shift, $g(T)$-g_0, increase proportional to the particle magnetic moments determined from the Langevin analysis of the magnetization isotherms. These features are explained by the scattering of the $q\rightarrow 0$ magnon from an electron-hole (e/h) pair mediated by the spin-orbit coupling, while the *sd* exchange can be ruled out. The large saturation values, $\alpha(0)=0.76$ and $g(0)/g_0-1=-0.37$, indicate the dominance of an overdamped 1 meV e/h pair which seems to originate from the discrete levels of the itinerant electrons in the $d_p=3$ nm nanoparticles.

DOI: 10.1103/PhysRevB.76.104404 PACS number(s): 76.50.+g, 78.67.Bf

I. INTRODUCTION

The ongoing downscaling of magneto electronic devices maintains the yet intense research of spin dynamics in ferromagnetic structures with restricted dimensions. The effect of surfaces, interfaces, and disorder in ultrathin films,[1] multilayers, and nanowires[2] has been examined and discussed in great detail. On structures confined to the nm scale in all three dimensions, like ferromagnetic nanoparticles, the impact of anisotropy[3] and particle-particle interactions[4] on the Neél-Brown-type dynamics, which controls the switching of the longitudinal magnetization, is now also well understood. On the other hand, the dynamics of the transverse magnetization, which, e.g., determines the externally induced, ultrafast magnetic switching in ferromagnetic nanoparticles, is still a topical issue. Such fast switching requires a large, i.e., a critical value of the Landau-Lifshitz-Gilbert (LLG) damping parameter α.[5] This damping has been studied by conventional[6,7] and, more recently, by advanced[8] ferromagnetic resonance (FMR) techniques, revealing enhanced values of α up to the order of one.

By now, the LLG damping of bulk ferromagnets is almost quantitatively explained by the scattering of the $q=0$ magnon by conduction electron-hole (e/h) pairs due to the spin-orbit coupling Ω_{so}.[9] According to recent *ab initio* band-structure calculations,[10] the rather small values for $\alpha\approx\Omega_{so}^2\tau$ result from the small (Drude) relaxation time τ of the electrons. For nanoparticles, the Drude scattering and also the wave-vector conservation are ill-defined, and *ab initio* many-body approaches to the spin dynamics should be more appropriate. Numerical work by Cehovin *et al.*[11] considers the modification of the FMR spectrum by the discrete level structure of the itinerant electrons in the particle. However, the effect of the resulting electron-hole excitation, $\epsilon_p\sim v_p^{-1}$, where v_p is the nanoparticle volume on the intrinsic damping has not yet been considered.

Here we present FMR spectra recorded at $\omega/2\pi=9.1$ GHz on $Fe_{0.2}Pt_{0.8}$ nanospheres, the structural and magnetic properties of which are summarized in Sec. II. In Sec. III the measured FMR shapes will be examined by solutions of the LLG equation of motion for the particle moments. Several effects, in particular those predicted for crystalline anisotropy[12] and superparamagnetic (SPM) fluctuations of the particle moments[13] will be considered. In Sec. IV, the central results of this study, i.e., the LLG-damping $\alpha(T)$ reaching values of almost 1 and a large g-shift, $g(T)$-g_0, are presented. Since both $\alpha(T)$ and $g(T)$ increase proportional to the particle magnetization, they can be related to spin-orbit damping torques, which, due to the large values of α and Δg are rather strongly correlated. It will be discussed which features of the e/h excitations are responsible for these correlations in a nanoparticle. A summary and the conclusions are given in the final section.

II. NANOPARTICLE CHARACTERIZATION

The nanoparticle assembly has been prepared[14] following the wet-chemical route by Sun *et al.*.[15] In order to minimize the effect of particle-particle interactions, the nanoparticles were highly dispersed.[14] Transmission electron microscopy revealed nearly spherical shapes with mean diameter $d_p=3.1$ nm and a rather small width of the log-normal size distribution, $\sigma_d=0.17(3)$. Wide angle x-ray diffraction provided the chemically disordered fcc structure with a lattice constant $a_0=0.3861$ nm.[14]

The mean magnetic moments of the nanospheres $\mu_p(T)$ have been extracted from fits of the magnetization isotherms $M(H,T)$, measured by a SQUID magnetometer (Quantum Design, MPMS2) in units emu/g$=1.1\times10^{20}$ μ_B/g, to

$$M_L(H,T)=N_p\mu_p(T)\mathcal{L}\left(\frac{\mu_pH}{k_BT}\right). \quad (1)$$

Here, $\mathcal{L}(y)=\coth(y)-y^{-1}$ with $y=\mu_p(T)H/k_BT$ is the Langevin function and N_p is the number of nanoparticles per gram. The fits shown in Fig. 1(a) demanded for a small paramagnetic background, $M-M_L=\chi_b(T)H$, with a strong Curie-type temperature variation of the susceptibility χ_b, signalizing the presence of paramagnetic impurities. According to the inset of Fig. 1(b) this $1/T$ law turns out to agree with the tempera-

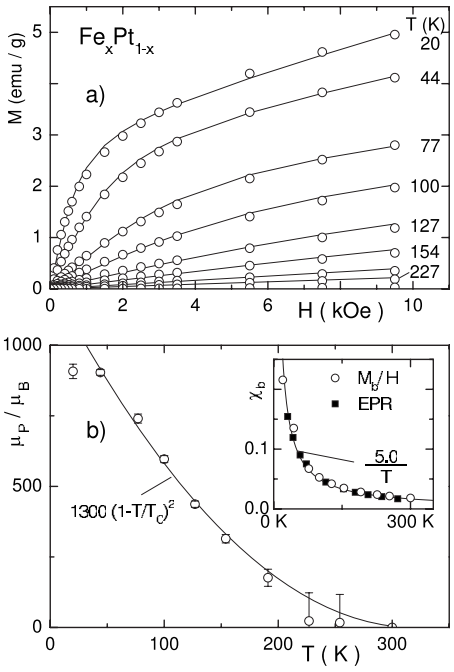

FIG. 1. (a) Magnetization isotherms of the nanospheres fitted to the Langevin model plus a small paramagnetic background $\chi_b H$; (b) temperature dependences of the magnetic moments of the nanoparticles μ_p and of the background susceptibility χ_b (inset units are emu/g kOe) fitted to the indicated relations with $T_C=(320\pm20)$ K. The inset shows also data from the intensity of the electron paramagnetic resonance (EPR) at 1.45 kOe, see Figs. 2 and 3.

ture dependence of the intensity of a weak, narrow magnetic resonance with $g_i=4.3$ depicted in Figs. 2 and 3. Such narrow line with the same g factor has been observed by Berger *et al.*[16] on partially crystallized iron-containing borate glass and could be traced to isolated Fe^{3+} ions.

The results for $\mu_p(T)$ depicted in Fig. 1(b) show the moments to saturate at $\mu_p(T\to0)=(910\pm30)\mu_B$. This yields a mean moment per atom in the fcc unit cell of $\bar{\mu}(0)=\mu_p a_0^3/4v_p=0.7\mu_B$ corresponding to a spontaneous magnetization $M_s(0)=5.5$ kOe. According to previous work by Menshikov *et al.*[17] on chemically disordered Fe_xPt_{1-x} this corresponds to an iron concentration of $x=0.20$. Upon rising temperature the moments decrease rapidly, which above 40 K can be rather well parametrized by the empirical power law, $\mu_p(T\geq40\text{ K})\sim(1-T/T_C)^\beta$ revealing $\beta=2$ and for the Curie temperature $T_C=(320\pm20)$ K. This is consistent with $T_C=(310\pm10)$ K for $Fe_{0.2}Pt_{0.8}$ emerging from a slight extrapolation of results for $T_C(x\geq0.25)$ of Fe_xPt_{1-x}.[18] No quantitative argument is at hand for the exponent $\beta=2$, which is much larger than the mean-field value $\beta_{MF}=1/2$. We believe that $\beta=2$ may arise from a reduced thermal stability of the magnetization due to strong fluctuations of the ferromagnetic exchange between Fe and Pt in the disordered structure and also to additional effects of the antiferromagnetic Fe-Fe and Pt-Pt exchange interactions. In this context, it may be interesting to note that for low Fe concentrations, $x\leq0.3$, bulk Fe_xPt_{1-x} exhibits ferromagnetism only in the disordered structure,[17] while structural ordering leads to paraferromagnetism or antiferromagnetism. Recent first-principle calculations of the electronic structure produced clear evidence for the stabilizing effect of disorder on the ferromagnetism in FePt.[19]

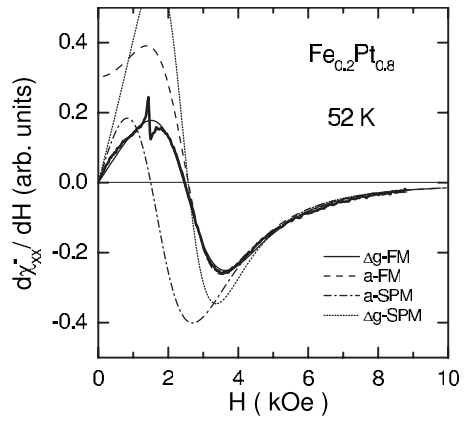

FIG. 2. (a) Derivative of the microwave ($f=9.095$ GHz) absorption spectrum recorded at $T=52$ K, i.e., close to magnetic saturation of the nanospheres. The solid and dashed curves are based on fits to Eqs. (4) and (8), respectively, which both ignore SPM fluctuations and assume either a g-shift and zero anisotropy field H_A (Δg-FM) or $\Delta g=0$ and a randomly distributed $H_A=0.5$ kOe (a-FM), Eq. (9). Also shown are fits to predictions by Eq. (11), which account for SPM fluctuations, with $H_A=0.5$ kOe and $\Delta g=0$ (a-SPM) and, using Eq. (11), for $\Delta g\neq0$ and $H_A=0$ (Δg-SPM). The weak, narrow resonance at 1.45 kOe is attributed to the paramagnetic background with $g=4.3\pm0.1$ indicating Fe^{3+} (Ref. 16) impurities.

From the Langevin fits in Fig. 1(a) we obtain for the particle density $N_p=3.5\times10^{17}$ g^{-1}. Based on the well-known mass densities of $Fe_{0.2}Pt_{0.8}$ and the organic matrix, we find by a little calculation[20] for the volume concentration of the particles $c_p=0.013$ and, hence, for the mean interparticle distance, $d_{pp}=d_p/c_p^{1/3}=13.5$ nm. This implies for the maximum (i.e., $T=0$) dipolar interaction between nearest particles, $\mu_p^2(0)/4\pi\mu_0 d_{pp}^3=0.20$ K, so that at the present temperatures, $T\geq20$ K, the sample should act as an ensemble of indepen-

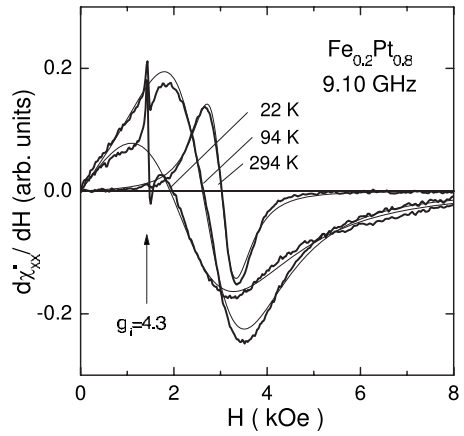

FIG. 3. Derivative spectra at some representative temperatures and fits to Eq. (4). The LLG-damping, g-shift, and intensities are depicted in Fig. 4.

dent ferromagnetic nanospheres. Since also the blocking temperature, $T_b=9$ K, as determined from the maximum of the ac susceptibility at 0.1 Hz in zero magnetic field,[20] turned out to be low, the Langevin analysis in Fig. 1(a) is valid.

III. RESONANCE SHAPE

Magnetic resonances at a fixed *X*-band frequency of 9.095 GHz have been recorded by a homemade microwave reflectometer equipped with field modulation to enhance the sensitivity. A double-walled quartz tube containing the sample powder has been inserted to a multipurpose, gold-plated VARIAN cavity (model V-4531). Keeping the cavity at room temperature, the sample could be either cooled by means of a continuous flow cryostat (Oxford Instruments, model ESR 900) down to 15 K or heated up to 500 K by an external Pt-resistance wire.[20] At all temperatures, the incident microwave power was varied in order to assure the linear response.

Some examples of the spectra recorded below the Curie temperature are shown in Figs. 2 and 3. The spectra have been measured from −9.5 kOe to +9.5 kOe and proved to be independent of the sign of H and free of any hysteresis. This can be expected due to the completely reversible behavior of the magnetization isotherms above 20 K and the low blocking temperature of the particles. Lowering the temperature, we observe a downward shift of the main resonance accompanied by a strong broadening. On the other hand, the position and width of the weak narrow line at (1.50 ± 0.05) kOe corresponding to $g_i\cong4.3$ remain independent of temperature. This can be attributed to the previously detected paramagnetic Fe^{3+} impurities[16] and is supported by the integrated intensity of this impurity resonance $I_i(T)$ evaluated from the amplitude difference of the derivative peaks. Since the intensity of a paramagnetic resonance is given by the paramagnetic susceptibility, $I_i(T)\sim\int dH\chi''_{xx}(H,T)\sim\chi_i(T)$ can be compared directly to the background susceptibility $\chi_b(T)$, see inset to Fig. 1(b). The good agreement between both temperature dependencies suggests to attribute χ_b to these Fe^{3+} impurities. An analysis of the fitted Curie constant, $C_i=5$ emu K/g kOe, yields $N_i=164\times10^{17}$ g^{-1} for the Fe^{3+} concentration, which corresponds to 50 Fe^{3+} per 1150 atoms of a nanosphere.

With regard to the main intensity, we want to extract the maximum-possible information, in particular, on the intrinsic magnetic damping in nanoparticles. Unlike the conventional analysis of resonance fields and linewidths, as applied, e.g., to Ni[6] and Co[7] nanoparticles, our objective is a complete shape analysis in order to disentangle effects by the crystalline anisotropy,[12] by SPM fluctuations,[13] by an electronic *g*-shift,[21] and by different forms of the damping torque $\vec{R}$.[22] Additional difficulties may enter the analysis due to nonspherical particle shapes, size distributions and particle interaction, all of which, however, can be safely excluded for the present nanoparticle assembly.

The starting point of most FMR analyses is the phenomenological equation of motion for a particle moment (see, e.g., Ref. 13)

$$\frac{d}{dt}\vec{\mu}_p=\gamma\vec{H}_{\rm eff}\times\vec{\mu}_p-\vec{R}, \tag{2}$$

using either the original Landau-Lifshitz (LL) damping with damping frequency λ_L,

$$\vec{R}_L=\frac{\lambda_L}{M_s}(\vec{H}_{\rm eff}\times\vec{\mu}_p)\times\vec{s}_p, \tag{3}$$

or the Gilbert damping with the Gilbert damping parameter α_G,

$$\vec{R}_G=\alpha_G\frac{d\vec{\mu}_p}{dt}\times\vec{s}_p, \tag{4}$$

where $\vec{s}_p=\vec{\mu}_p/\mu_p$ denotes the direction of the particle moment. In Eq. (2), the gyromagnetic ratio, $\gamma=g_0\mu_B/\hbar$, is determined by the regular *g*-factor g_0 of the precessing moments. It should perhaps be noted that the validity of the micromagnetic approximation underlying Eq. (2) has been questioned[23] for volumes smaller than $[2\lambda_{\rm sw}(T)]^3$, where $\lambda_{\rm sw}=2a_0T_C/T$ is the smallest wavelength of thermally excited spin waves. For the present particles, this estimate leads to a fairly large temperature of $\sim0.7T_C$ up to which micromagnetics should hold.

At first, we ignore the anisotropy being small in cubic Fe_xPt_{1-x},[24,25] so that for the present nanospheres the effective field is identical to the applied field, $\vec{H}_{\rm eff}=\vec{H}$. Then, the solutions of Eq. (2) for the susceptibility of the two normal, i.e., circularly polarized modes, of N_p independent nanoparticles per gram take the simple forms

$$\chi^L_\pm(H)=N_p\mu_p\gamma\frac{1\mp i\alpha}{\gamma H(1\mp i\alpha)\mp\omega} \tag{5}$$

for $\vec{R}=\vec{R}_L$ with $\alpha=\lambda_L/\gamma M_s$ and for the Gilbert torque $\vec{R}_G$,

$$\chi^G_\pm(H)=N_p\mu_p\gamma\frac{1}{\gamma H\mp\omega(1+i\alpha_G)}. \tag{6}$$

For the LL damping, the experimental, transverse susceptibility, $\chi_{xx}=\frac{1}{2}(\chi_++\chi_-)$, takes the form

$$\chi^L_{xx}(H)=N_p\mu_p\gamma\frac{\gamma H(1+\alpha^2)-i\alpha\omega}{(\gamma H)^2(1+\alpha^2)-\omega^2-2i\alpha\omega\gamma H}. \tag{7}$$

As the same shape is obtained for the Gilbert torque with $\alpha=\alpha_G$, the damping is frequently denoted as the LLG parameter. However, the gyromagnetic ratio in Eq. (7) must be replaced by $\gamma/(1+\alpha^2)$, which only for $\alpha\ll1$ implies also the same resonance field H_r. Upon increasing the damping up to $\alpha\approx0.7$ (the regime of interest here), the resonance field H_r of $\chi^G_{xx}(H)$, determined by $d\chi''/dH=0$, remains constant, $H^G_r\approx\omega/\gamma$, while H^L_r decreases rapidly. After renormalization $\gamma/(1+\alpha^2)$ the resonance fields and also the shapes of $\chi^L(H)$ and $\chi^G(H)$ become identical. This effect should be observed when determining the *g* factor from the resonance fields of broad lines. It becomes even more important if the downward shift of H_r is attributed to anisotropy, as done recently for the rather broad FMR absorption of Fe_xPt_{1-x} nanoparticles with larger Fe content, $x\geq0.3$.[26]

In order to check here for both damping torques, we selected the shape measured at a low temperature, $T=52$ K, where the linewidth proved to be large (see Fig. 2) and the magnetic moment $\mu_p(T)$ was close to saturation [Fig. 1(b)]. Neither of the damping terms could explain both, the observed resonance field H_r and the linewidth $\Delta H=\alpha\omega/\gamma$, and, hence, the line shape. By using $\vec{R}_G$, the shift of H_r from $\omega/\gamma=3.00$ kOe was not reproduced by $H_r^G=\omega/\gamma$, while for $\vec{R}_L$ the resonance field H_r^L, demanded by the linewidth, became significantly smaller than H_r.

This result suggested to consider as next the effect of a crystalline anisotropy field $\vec{H}_A$ on the transverse susceptibility, which has been calculated by Netzelmann from the free energy of a ferromagnetic grain.[12] Specializing his general ansatz to a uniaxial $\vec{H}_A$ oriented at angles (θ,ϕ) with respect to the dc field $\vec{H}\|\vec{e}_z$ and the microwave field, one obtains by minimizing

$$F(\theta,\phi,\vartheta,\varphi)=-\mu_p\left\{H\cos\vartheta+\frac{1}{2}H_A[\sin\vartheta\sin\theta-\cos(\varphi-\phi)+\cos\theta\cos\vartheta]^2\right\} \tag{8}$$

the equilibrium orientation (ϑ_0,φ_0) of the moment $\vec{\mu}_p$ of a spherical grain. After performing the trivial average over ϕ, one finds for the transverse susceptibility of a particle with orientation θ,

$$\chi_{xx}^L(\theta,H)=\frac{\gamma\mu_p}{2}\frac{(F_{\vartheta_0\vartheta_0}+F_{\varphi_0\varphi_0}/\tan^2\vartheta_0)(1+\alpha^2)-i\alpha\mu_p\omega(1+\cos^2\vartheta_0)}{(1+\alpha^2)(\gamma H_{\mathrm{eff}})^2-\omega^2-i\alpha\omega\gamma\Delta H}. \tag{9}$$

Here $H_{\mathrm{eff}}^2=[F_{\vartheta_0\vartheta_0}F_{\varphi_0\varphi_0}-F_{\vartheta_0\varphi_0}^2/(\mu_p\sin\vartheta_0)^2]$ and $\Delta H=(F_{\vartheta_0\vartheta_0}+F_{\varphi_0\varphi_0}/\sin^2\vartheta_0)/\mu_p$ are given by the second derivatives of F at the equilibrium orientation of $\vec{\mu}_p$. For the randomly distributed $\vec{H}_A$ of N_p independent particles per gram one has

$$\chi_{xx}^L(H)=\int_0^{\pi/2}d(\cos\theta)\chi_{xx}^L(\theta,H). \tag{10}$$

In a strict sense, this result should be valid at fields larger than the so-called thermal fluctuation field $H_T=k_BT/\mu_p(T)$, see, e.g., Ref. 13, which for the present case amounts to $H_T=1.0$ kOe. Hence, in Fig. 2 we fitted the data starting at high fields, reaching there an almost perfect agreement with the curve a-FM. The fit yields a rather small $H_A=0.5$ kOe which implies a small anisotropy energy per atom, $E_A=\frac{1}{2}\mu_p(0)H_A=1.0$ μeV. This number is smaller than the calculated value for bulk fcc FePt, $E_A=4.0$ μeV,[25] most probably due to the lower Fe concentration ($x=0.20$) and the strong structural disorder in our nanospheres. We emphasize, that the main defect of this a-FM fit curve arises from the finite value of $d\chi_{xx}''/dH$ at $H=0$. By means of Eq. (9) one finds $\chi_{xx}''(H\to 0,\theta)\sim H_AH/\omega^2$,which remains finite even after averaging over all orientations according to θ [Eq. (10)].

The finite value of the derivative of $\chi_{xx}''(H\to 0)$ should disappear if superparamagnetic (SPM) fluctuations of the particles are taken into account. Classical work[27] predicted the anisotropy field to be reduced by SPM, $H_A(y)=H_A[1/L(y)-3/y]$, which for $y=H/H_T\ll 1$ implies $H_A(y)=H_Ay/5$ and, therefore, $\chi_{xx}''(H\to 0)\sim H^2$. A statistical theory for $\chi_{xx}^L(H,T)$ which considers the effect of SPM fluctuations exists only to first order in H_A/H.[21] The result of this linear model (LM) in H_A/H which generalizes Eq. (4), can be cast in the form

$$\chi_{\pm}^{\mathrm{LM}}(\theta,H)=N_p\mu_p\gamma L(y)\frac{(1+A\mp i\alpha_A)}{\gamma(1+B\mp i\alpha_B)H\mp\omega}. \tag{11}$$

The additional parameters are given in Ref. 21 and contain, depending on the symmetry of H_A, higher-order Langevin functions $L_j(y)$ and their derivatives. Observing the validity of the LM for $H\gg H_A=0.5$ kOe, we fitted the data in Fig. 2 to Eq. (11) with $\chi_{xx}^{\mathrm{LM}}(\theta,H)=\frac{1}{2}(\chi_+^{\mathrm{LM}}+\chi_-^{\mathrm{LM}})$ at larger fields. There, one has also $H\gg H_T=1.0$ kOe and the fit, denoted as a-SPM, agrees with the ferromagnetic result (a-FM). However, increasing deviations appear below fields of 4 kOe. By varying H_A and α, we tried to improve the fit near the resonance $H_r=2.3$ kOe and obtained unsatisfying results. For low anisotropy, $H_A\leq 3$ kOe, the resonance field could be reproduced only by significantly lower values of α, which are inconsistent with the measured width and shape. For $H_A>3$ kOe, a small shift of H_r occurs, but at the same time the line shape became distorted, tending to a two-peak structure also found in previous simulations.[13] Even at the lowest temperature, $T=22$ K, where the thermal field drops to $H_T=0.4$ kOe, no signatures of such inhomogeneous broadening appear (see Fig. 3). Finally, it should be mentioned that all of the above attempts to incorporate the anisotropy in the discussion of the line shape were based on the simplest nontrivial, i.e., uniaxial symmetry, which for FePt was also considered by the theory.[25] For cubic anisotropy, the same qualitative discrepancies were found in our simulations.[20] This insensitivity with respect to the symmetry of H_A originates from the orientational averaging in the range of the H_A values of relevance here.

As a finite anisotropy failed to reproduce H_r, ΔH, and also the shape, we tried the ansatz for the magnetic resonance of nanoparticles by introducing a complex LLG parameter,

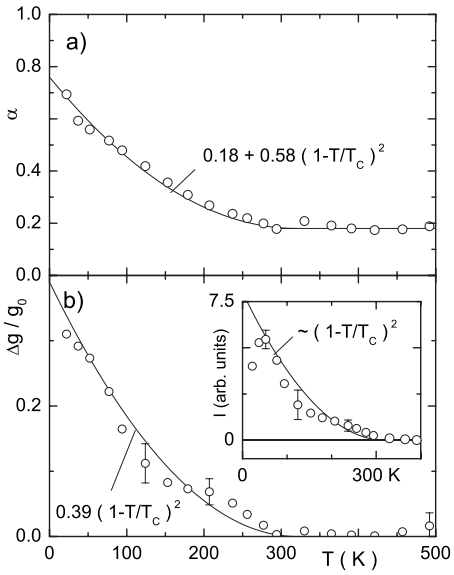

FIG. 4. Temperature variation (a) of the LLG damping α and (b) of the relative g-shifts with $g_0=2.16$ (following from the resonance fields at $T>T_C$). Within the error margins, $\alpha(T)$ and $\Delta g(T)$ and also the fitted intensity of the LLG shape (see inset) display the same temperature dependence as the particle moments in Fig. 1(b).

$$\hat{\alpha}(T) = \alpha(T) - i\beta(T). \tag{12}$$

According to Eq. (4) this is equivalent to a negative g-shift, $g(T)-g_0=-\beta(T)g_0$, which is intended to compensate for the too large downward shift of H_r^L demanded by $\chi_{xx}^L(H)$ due to the large linewidth. In fact, inserting this ansatz in Eq. (5), the fit, denoted as Δg-FM in Fig. 2, provides a convincing description of the line shape down to zero magnetic field. It may be interesting to note that the resulting parameters, $\alpha=0.56$ and $\beta=0.27$, revealed the same shape as obtained by using the Gilbert susceptibilities, Eq. (6).

In spite of the agreement of the Δg-FM model with the data, we also tried to include here SPM fluctuations by using $\hat{\alpha}(T,H)=\hat{\alpha}(T)[1/L(y)-1/y]$ (Ref. 21) for $H_A=0$. The result, designated as Δg-SPM in Fig. 2 agrees with the Δg-FM curve for $H \gg H_T$ where $\hat{\alpha}(T,H)=\hat{\alpha}(T)$, but again significant deviations occur at lower fields. They indicate that SPM fluctuations do not play any role here, and this conclusion is also confirmed by the results at higher temperatures. There, the thermal fluctuation field, $H_T=k_BT/\mu_p(T)$, increases to values larger than the maximum measuring field, $H=10$ kOe, so that SPM fluctuations should cause a strong thermal, homogeneous broadening of the resonance due to $\hat{\alpha}(H \gg H_T) = \hat{\alpha}2H_T/H$. However, upon increasing temperature, the fitted linewidths, (Fig. 3) and damping parameters (Fig. 4) display the reverse behavior.

IV. COMPLEX DAMPING

In order to shed more light on the magnetization dynamics of the nanospheres we examined the temperature variation of the FMR spectra. Figure 3 shows some examples recorded below the Curie temperature, $T_C=320$ K, together with fits to the a-FM model outlined in the preceding section. Above T_C, the resonance fields and the linewidths are temperature independent revealing a mean g factor, $g_0=2.16\pm0.02$, and a damping parameter $\Delta H/H_r=\alpha_0=0.18\pm0.01$. Since g_0 is consistent with a recent report on g values of Fe_xPt_{1-x} for $x \geq 0.43$,[21] we suspect that this resonance arises from small Fe_xPt_{1-x} clusters in the inhomogeneous $Fe_{0.2}Pt_{0.8}$ structure. Fluctuations of g_0 and of local fields may be responsible for the rather large width. This interpretation is supported by the observation that above T_C the line shape is closer to a Gaussian than to the Lorentzian following from Eq. (7) for small α.

The temperature variation for both components of the complex damping, obtained from the fits below T_C to Eq. (7), are shown in Fig. 4. Clearly, they obey the same power law as the moments, $\mu_p(T)$, displayed in Fig. 1(b), which implies

$$\hat{\alpha}(T) = (\alpha - i\beta)m_s(T) + \alpha_0. \tag{13}$$

Here $m_s(T)=\mu_p(T)/\mu_p(0)$, $\alpha=0.58$, and $\beta=-\Delta g(0)/g_0=0.39$ denote the reduced spontaneous magnetization and the saturation values for the complex damping, respectively. It should be emphasized that the fitted intensity $I(T)$ of the spectra, shown by the inset to Fig. 4(b), exhibits the same temperature variation $I(T) \sim \mu_p(T)$. This behavior is predicted by the ferromagnetic model, Eq. (7), and is a further indication for the absence of SPM effects on the magnetic resonance. If the resonance were dominated by SPM fluctuations, the intensity should decrease like the SPM Curie susceptibility, $I_{SPM}(T) \sim \mu_p^2(T)/T$, following from Eq. (11), being much stronger than the observed $I(T)$.

At the beginning of a physical discussion of $\hat{\alpha}(T)$, we should point out that the almost perfect fits of the line shape to Eq. (7) indicate that the complex damping is related to an intrinsic mechanism and that eventual inhomogeneous effects by distributions of particle sizes and shapes in the assembly, as well as by structural disorder are rather unlikely. Since a general theory of the magnetization dynamics in nanoparticles is not yet available, we start with the current knowledge on the LLG damping in bulk and thin film ferromagnets, as recently reviewed by Heinrich.[5] Based on experimental work on the archetypal metallic ferromagnets and on recent *ab initio* band-structure calculations[10] there is now rather firm evidence that the damping of the $q=0$ magnon is associated with the torques $\vec{T}_{so}=\vec{m}_s \times \Sigma_j(\xi_j \vec{L}_j \times \vec{S})$ on the spin $\vec{S}$ due to the spin-orbit interaction ξ_j at the lattice sites j. The action of the torque is limited by the finite lifetime τ of an e/h excitation, the finite energy ϵ of which may cause a phase, i.e., a g-shift. As a result of this magnon-e/h-pair scattering, the temperature-dependent part of the LLG damping parameter becomes

$$\hat{\alpha}(T) - \alpha_0 = \frac{\lambda_L(T)}{\gamma M_s(T)} = \frac{[\Omega_{so} m_s(T)]^2}{\tau^{-1} + i\epsilon/\hbar} \frac{1}{\gamma M_s(T)}. \tag{14}$$

For intraband scattering, $\epsilon \ll \hbar/\tau$, the aforementioned numerical work[10] revealed $\Omega_{so}=0.8\times10^{11}$ s^{-1} and 0.3×10^{11} s^{-1} as effective spin-orbit coupling in fcc Ni and bcc Fe, respectively. Hence, the narrow unshifted ($\Delta g=0$) bulk FMR lines in pure crystals, where $\alpha \leq 10^{-2}$, are related to

intraband scattering with $\epsilon \ll \hbar/\tau$ and to electronic (momentum) relaxation times τ smaller than 10^{-13} s.

Following Eq. (14), we discuss at first the temperature variation, which implies a linear dependence, $\hat{\alpha}(T)-\alpha_0 \sim m_s(T)$. Obviously, both, the real and imaginary part of $\hat{\alpha}(T)-\alpha_0$, agree perfectly with the fits to the data in Fig. 4, if the relaxation time τ remains constant. It may be interesting to note here that the observed temperature variation of the complex damping $\lambda_L(T)$ is not predicted by the classical model[28] incorporating the *sd*-exchange coupling J_{sd}. According to this model, which has been advanced recently to ferromagnets with small spin-orbit interaction[29] and ferromagnetic multilayers,[30] J_{sd} transfers spin from the localized 3*d* moments to the delocalized *s*-electron spins within their spin-flip time τ_{sf}. From the mean-field treatment of their equations of motion by Turov,[31] we find a form analogous to Eq. (14),

$$\alpha_{sd}(T) = \frac{\Omega_{sd}^2 \chi_s}{\tau_{sf}^{-1} + i\tilde{\Omega}_{sd}} \frac{1}{\gamma M_s(T)}, \tag{15}$$

where $\Omega_{sd}=J_{sd}/\hbar$ is the exchange frequency, χ_s the Pauli susceptibility of the *s* electrons, and $\tilde{\Omega}_{sd}/\Omega_{sd}=(1+\Omega_{sd}\chi_s/\gamma M_d)$. The same form follows from more detailed considerations of the involved scattering process (see, e.g., Ref. 5). As a matter of fact, the LLG damping $\alpha_{sd}=\lambda_{sd}/\gamma M_d$ cannot account for the observed temperature dependence, because Ω_{sd} and χ_s are constants. The variation of the spin torques with the spontaneous magnetization $m_s(T)$ drops out in this model, since the *sd* scattering involves transitions between the 3*d* spin-up and spin-down bands due to the splitting by the exchange field $J_{sd}\, m_s(T)$.

By passing from the bulk to the nanoparticle ferromagnet, we use Eq. (14) to discuss our results for the complex $\hat{\alpha}(T)$, Eq. (13). Recently, for Co nanoparticles with diameters 1–4 nm, the existence of a discrete level structure near ϵ_F has been evidenced,[32] which suggests to associate the e/h energy ϵ with the level difference ϵ_p at the Fermi energy. From Eqs. (13) and (14) we obtain relations between ϵ and the lifetime of the e/h pair and the experimental parameters α and β,

$$\tau^{-1} = \frac{\alpha}{\beta}\frac{\epsilon}{\hbar}, \tag{16a}$$

$$\frac{\epsilon}{\hbar} = \frac{\beta}{\alpha^2+\beta^2}\frac{\Omega_{so}^2}{\gamma M_s(0)}. \tag{16b}$$

Due to $\alpha/\beta=1.5$, Eq. (16a) reveals a strongly overdamped excitation, which is a rather well-founded conclusion. The evaluation of ϵ, on the other hand, depends on an estimate for the effective spin-orbit coupling, $\Omega_{so}=\eta_L\chi_e^{1/2}\xi_{so}/\hbar$ where η_L represents the matrix element of the orbital angular momentum between the e/h states.[5] The spin-orbit coupling of the minority Fe spins in FePt has been calculated by Sakuma,[24] $\xi_{so}=45$ meV, while the density of states $\mathcal{D}(\epsilon_F) \approx 1/(\text{eV atom})$ (Refs. 24 and 33) yields a rather high susceptibility of the electrons, $\eta_L\chi_e=\mu_B^2\mathcal{D}(\epsilon_F)=4.5\times10^{-5}$. Assuming $\eta_L=1$, both results lead to $\Omega_{so}\approx 3.5\times10^{11}$ s^{-1}, which is by one order of magnitude larger than the values for Fe and Ni mentioned above. One reason for this enhancement and for a large matrix element, $\eta_L=1$, may be the strong hybridization between 3*d* and 4*d* Pt orbitals[24] in Fe_xPt_{1-x}. By inserting this result into Eq. (16b) we find $\epsilon=0.8$ meV. In fact, this value is comparable to an estimate for the level difference at ϵ_F,[32] $\epsilon_p=[\mathcal{D}(\epsilon_F)N_p]^{-1}$ which for our particles with $N_p=(2\pi/3)(d_p/a_0)^3=1060$ atoms yields $\epsilon_p=0.9$ meV. Regarding the several involved approximations, we believe that this good agreement between the two results on the energy of the e/h excitation, $\epsilon \approx \epsilon_p$, may be accidental. However, we think, that this analysis provides a fairly strong evidence for the magnon scattering by this excitation, i.e., for the gap in the electronic states due to confinement of the itinerant electrons to the nanoparticle.

V. SUMMARY AND CONCLUSIONS

The analysis of magnetization isotherms explored the mean magnetic moments of $Fe_{0.2}Pt_{0.8}$ nanospheres ($d_p=3.1$ nm) suspended in an organic matrix, their temperature variation up to the Curie temperature T_C, the large mean particle-particle distance $D_{pp} \gg d_p$, and the presence of Fe^{3+} impurities. Above T_C, the resonance field H_r of the 9.1 GHz microwave absorption yielded a temperature independent mean *g* factor, $g_0=2.16$, consistent with a previous report[21] for paramagnetic Fe_xPt_{1-x} clusters. There, the line shape proved to be closer to a Gaussian with rather large linewidth, $\Delta H/H_r=0.18$, which may be associated with fluctuations of g_0 and local fields both due to the chemically disordered fcc structure of the nanospheres.

Below the Curie temperature, a detailed discussion of the shape of the magnetic resonance spectra revealed a number of unexpected features.

(i) Starting at zero magnetic field, the shapes could be described almost perfectly up to highest field of 10 kOe by the solution of the LLG equation of motion for independent ferromagnetic spheres with negligible anisotropy. Signatures of SPM fluctuations on the damping, which have been predicted to occur below the thermal field $H_T=k_BT/\mu_p(T)$, could not be realized.

(ii) Upon decreasing temperature, the LLG damping increases proportional to $\mu_p(T)$, i.e., to the spontaneous magnetization of the particles, reaching a rather large value $\alpha=0.7$ for $T \ll T_C$. We suspect that this high intrinsic damping may be responsible for the absence of the predicted SPM effects on the FMR, since the underlying statistical theory[13] has been developed for $\alpha \ll 1$. This conjecture may further be based on the fact that the large intrinsic damping field $\Delta H=\alpha\omega/\gamma=2.1$ kOe causes a rapid relaxation of the transverse magnetization ($q=0$ magnon) as compared to the effect of statistical fluctuations of H_T added to H_{eff} in the equation of motion, Eq. (2).[13]

(iii) Along with the strong damping, the line-shape analysis revealed a significant reduction of the *g* factor, which also proved to be proportional to $\mu_p(T)$. Any attempts to account for this shift by introducing uniaxial or cubic anisotropy fields failed, since low values of $\vec{H}_A$ had no effect on the

resonance field due to the orientational averaging. On the other hand, larger $\vec{H}_A$'s, by which some small shifts of H_r could be obtained, produced severe distortions of the calculated line shape.

The central results of this work are the temperature variation and the large magnitudes of both $\alpha(T)$ and $\Delta g(T)$. They were discussed by using the model of the spin-orbit induced scattering of the $q=0$ magnon by an e/h excitation ϵ, well established for bulk ferromagnets, where strong intraband scattering with $\epsilon \ll \hbar/\tau$ proved to dominate.[5] In nanoparticles, the continuous $\epsilon(\vec{k})$ spectrum of a bulk ferromagnet is expected to be split into discrete levels due to the finite number of lattice sites creating an e/h excitation ϵ_p. According to the measured ratio between damping and g-shift, this e/h pair proved to be overdamped, $\hbar/\tau_p = 1.5\epsilon_p$. Based on the free-electron approximation for ϵ_p (Ref. 32) and the density of states $\mathcal{D}(\epsilon_F)$ from band-structure calculations for Fe_xPt_{1-x},[24,33] one obtains a rough estimate $\epsilon_p \approx 0.9$ meV for the present nanoparticles. Using a reasonable estimate of the effective spin-orbit coupling to the minority Fe spins, this value could be well reproduced by the measured LLG damping, $\alpha=0.59$. Therefore, we conclude that the unexpected results of the dynamics of the transverse magnetization reported here are due to the presence of a broad e/h excitation with energy $\epsilon_p \approx 1$ meV. Deeper quantitative conclusions, however, must await more detailed information on the real electronic structure of nanoparticles near ϵ_F, which are also required to explain the overdamping of the e/h pairs, as it is inferred from our data.

ACKNOWLEDGMENTS

The authors are indebted to E. Shevchenko and H. Weller (Hamburg) for the synthesis and the structural characterization of the nanoparticles. One of the authors (J.K.) thanks B. Heinrich (Burnaby) and M. Fähnle (Stuttgart) for illuminating discussions.

[1] G. Woltersdorf, M. Buess, B. Heinrich, and C. H. Back, Phys. Rev. Lett. **95**, 037401 (2005); B. Koopmans, J. J. M. Ruigrok, F. Dalla Longa, and W. J. M. de Jonge, *ibid.* **95**, 267207 (2005); *Ultrathin Magnetic Structures III, IV*, edited by J. A. C. Bland and B. Heinrich (Springer-Verlag, Berlin, Heidelberg, New York, 2005).

[2] *Spin Dynamics in Confined Magnetic Structures III*, edited by B. Hillebrands and A. Thiaville (Springer-Verlag, Berlin, Heidelberg, New York, 2006).

[3] W. Wernsdorfer, E. B. Orozco, K. Hasselbach, A. Benoit, B. Barbara, N. Demoncy, A. Loiseau, H. Pascard, and D. Mailly, Phys. Rev. Lett. **78**, 1791 (1997); S. I. Woods, J. R. Kirtley, S. Sun, and R. H. Koch, *ibid.* **87**, 137205 (2001).

[4] C. Djurberg, P. Svedlindh, P. Nordblad, M. F. Hansen, F. Bødker, and S. Mørup, Phys. Rev. Lett. **79**, 5154 (1997); F. Luis, F. Petroff, J. M. Torres, L. M. García, J. Bartolomé, J. Carrey, and A. Vaurès, *ibid.* **88**, 217205 (2002).

[5] B. Heinrich, in *Ultrathin Magnetic Structures III*, edited by J. A. C. Bland and B. Heinrich (Springer-Verlag, Berlin, Heidelberg, New York, 2005), p. 143.

[6] V. K. Sharma and A. Baiker, J. Chem. Phys. **75**, 5596 (1981).

[7] M. Respaud, M. Goiran, J. M. Broto, F. H. Yang, T. O. Ely, C. Amiens, and B. Chaudret, Phys. Rev. B **59**, R3934 (1999).

[8] J. C. Sankey, P. M. Braganca, A. G. F. Garcia, I. N. Krivorotov, R. A. Buhrman, and D. C. Ralph, Phys. Rev. Lett. **96**, 227601 (2006); L. H. F. Andrade, A. Laraoui, M. Vomir, D. Muller, J.-P. Stoquert, C. Estournes, E. Beaurepaire, and J.-Y. Bigot, *ibid.* **97**, 127401 (2006).

[9] V. Korenman and R. E. Prange, Phys. Rev. B **6**, 2769 (1972).

[10] J. Kuneš and V. Kambersky, Phys. Rev. B **65**, 212411 (2002); **68**, 019901(E) (2003); D. Steiauf and M. Fähnle, *ibid.* **72**, 064450 (2005).

[11] A. Cehovin, C. M. Canali, and A. H. MacDonald, Phys. Rev. B **68**, 014423 (2003).

[12] U. Netzelmann, J. Appl. Phys. **68**, 1800 (1990).

[13] Yu. L. Raikher and V. I. Stepanov, Sov. Phys. JETP **75**, 764 (1992); Phys. Rev. B **50**, 6250 (1994).

[14] E. V. Shevchenko, D. Talapin, A. Kronowski, F. Wiekhorst, J. Kötzler, M. Haase, A. Rogach, and H. Weller, Adv. Mater. (Weinheim, Ger.) **14**, 287 (2002); E. Shevchenko, D. Talapin, A. Rogach, A. Kornowski, M. Haase, and H. Weller, J. Am. Chem. Soc. **124**, 11480 (2002).

[15] S. Sun, C. Murray, D. Weller, L. Folks, and A. Moser, Science **287**, 1989 (2000); S. H. Sun, E. E. Fullerton, D. Weller, and C. B. Murray, IEEE Trans. Magn. **37**, 1239 (2001); M. Nakaya, Y. Tsuchiya, K. Ito, Y. Oumi, T. Sano, and T. Teranishi, Chem. Lett. **33**, 130 (2004).

[16] R. Berger, J. Kliava, J.-C. Bissey, and V. Baïetto, J. Phys.: Condens. Matter **10**, 8559 (1998).

[17] A. Z. Menshikov, Yu. A. Dorofeev, V. A. Kazanzev, and S. K. Sidorov, Fiz. Met. Metalloved. **38**, 505 (1974).

[18] I. N. Nikolayev, B. V. Vinogradov, and L. S. Pavlynkov, Fiz. Met. Metalloved. **38**, 97 (1974).

[19] G. Brown, B. Kraczek, A. Janotti, T. C. Schulthess, G. M. Stocks, and D. D. Johnson, Phys. Rev. B **68**, 052405 (2003).

[20] F. Wiekhorst, D. Görlitz, and J. Kötzler (unpublished).

[21] M. Ulmeanu, C. Antoniak, U. Wiedwald, M. Farle, Z. Frait, and S. Sun, Phys. Rev. B **69**, 054417 (2004).

[22] R. Berger, J.-C. Bissey, and J. Kliava, J. Phys.: Condens. Matter **12**, 9347 (2000).

[23] N. Smith, J. Appl. Phys. **92**, 3877 (2002).

[24] A. Sakuma, J. Phys. Soc. Jpn. **63**, 3053 (1994).

[25] J. B. Staunton, L. Szunyogh, A. Buruzs, B. L. Gyorffy, S. Ostanin, and L. Udvardi, Phys. Rev. B **74**, 144411 (2006).

[26] F. Wiekhorst, E. Shevchenko, H. Weller, and J. Kötzler, J. Magn. Magn. Mater. **272-276**, 1559 (2004); C. Antoniak, J. Lindner, M. Spasova, D. Sudfeld, M. Acet, M. Farle, K. Fauth, U. Wiedwald, H.-G. Boyen, P. Ziemann, F. Wilhelm, A. Rogalev, and S. Sun, Phys. Rev. Lett. **97**, 117201 (2006).

[27] J. D. Livingston and C. P. Bean, J. Appl. Phys. **30**, S318 (1959); R. S. de Biasi and T. C. Devezas, *ibid.* **49**, 2466 (1978).

[28] B. Heinrich, D. Fraitova, and V. Kambersky, Phys. Status Solidi **23**, 501 (1967).
[29] Y. Tsnerkovnyak, G. A. Fiete, and B. I. Halperin, Appl. Phys. Lett. **84**, 5234 (2004).
[30] A. T. Costa, R. B. Muniz, and D. L. Mills, Phys. Rev. B **73**, 054426 (2006).
[31] E. A. Turov, in *Ferromagnetic Resonance*, edited by S. N. Vonsovski (Pergamon, Oxford, 1966), Chap. V, p. 7.
[32] S. Guéron, M. M. Deshmukh, E. B. Myers, and D. C. Ralph, Phys. Rev. Lett. **83**, 4148 (1999); S. Kleff, J. von Delft, M. M. Deshmukh, and D. C. Ralph, Phys. Rev. B **64**, 220401(R) (2001).
[33] E. T. Kulatov, Y.-A. Uspenskii, and S.-V. Halilov, J. Magn. Magn. Mater. **163**, 331 (1996).